

ROLE OF 3T MAGNETIC RESONANCE IMAGING IN EVALUATION OF BRACHIAL PLEXUS.

Dr. Aastha Agarwal¹, Dr. Varsha Rangankar², Dr. Reetika Kapoor^{3*}

¹Junior Resident, Department of Radiodiagnosis, Dr. D. Y. Patil Medical College, Hospital, and Research Centre, Dr. D Y Patil Vidyapeeth, Pimpri, Pune, India.

²Professor, Department of Radiodiagnosis, Dr. D. Y. Patil Medical College, Hospital, and Research Centre, Dr. D Y Patil Vidyapeeth, Pimpri, Pune, India.

^{3*}Junior resident, Department of Radiodiagnosis, Dr. D. Y. Patil Medical College, Hospital, and Research Centre, Dr. D Y Patil Vidyapeeth, Pimpri, Pune, India.

ABSTRACT

Aim: The aim of the present study was to assess the role of 3T Magnetic Resonance Imaging in evaluation of brachial plexus.

Methods: The Descriptive, cross-sectional study was conducted at Dr. D. Y. Patil Medical College and Hospital and Research Centre, Pimpri, Pune. Sixty-eight patients who had undergone brachial plexus MRI from August 2020 to September 2022 duration were included in the study.

Results: Out of 68 patients, the most common age group was 20-40 (55.9%) and majority were male patients (73.5%). Out of 68 patients, brachial plexus was found to be abnormal on MRI in 40 patients (58.8%) with unilateral involvement in 36 patients (90%) and bilateral involvement in 4 patients (10%). The most common pathology was brachial plexus injury, found in 25 cases (36.7%), followed by root compression in 9 cases (13.2%), parsonage turner syndrome in 5 cases (13.2%), primary brachial plexus tumors in 5 cases (7.3%) and secondary involvement of brachial plexus by metastases in 2 cases (2.9%). Fibrosis was seen in 3 cases (4.4%). On level wise analysis of brachial plexus involvement, the trunks were involved in 26 patients (38.2%), divisions were involved in 21 patients (30.9%), cords were involved in 22 patients (32.4%) and terminal branches were involved in 19 patients (27.9%). Pre-ganglionic root injury was found in 3 cases (4.4%), while 8 cases each of post-ganglionic root injury (11.7%) and pre plus post-ganglionic root injury (11.7%) were seen. On MRI and NVC/EMG correlation, MRI was found to be 94.7% sensitive and 90% specific for brachial plexopathies.

Conclusion: 3T MRI of brachial plexus provides valuable information regarding the morphology, location and extent of both traumatic and non-traumatic brachial plexopathies.

Keywords: Brachial plexus, injury, preganglionic, postganglionic, mass, fibrosis, Parsonage Turner syndrome.

INTRODUCTION

The brachial plexus is the primary source of motor and sensory innervation to the upper extremities. It originates from the ventral rami of the C5 to C8 and T1 nerves. As they pass through the supraclavicular fossa, the brachial plexus structures closely parallel the subclavian artery's course. They typically form three trunks, each of which divides into anterior and posterior divisions to create a total of six divisions. These six divisions then combine to form three cords. The roots and trunks are supraclavicular, while the divisions and cords are retro-clavicular and infraclavicular, respectively. Adult brachial plexopathy etiologies can be broadly categorized as either traumatic or non-traumatic. MRI is crucial in the identification, localization, and characterization of these causes and thus helps in their management. MRI of brachial plexus can be challenging due to the large field of view that must be covered with heterogeneous tissue distribution including muscles, fat and bones.^{1,2}

One percent of all major injuries are constituted by brachial plexus injuries (BPI), which can negatively impact upper-limb motor and sensory functioning and impair patients' quality of life.³ BPI often affects young people, primarily as a result of traffic accidents. The location and extent of the injury, as well as the time between the accident and the surgery, all affect the course of treatment and the prognosis for BPI.⁴ Therefore, in order to create a successful treatment strategy that can facilitate recovery from neurological symptoms, a clear diagnosis of the lesion is required.⁵

Clinical investigations, imaging studies, and electromyography are frequently used to diagnose BPI. However, clinical tests and electromyography play a limited role in assessing the location or extent of early-stage injury.⁶

Non-traumatic brachial plexopathies may result from systemic or diffuse causes, extrinsic compression, or infiltration by localized diseases. Neoplastic disease and radiation fibrosis are more frequent causes. Other reasons include genetic brachial plexopathy, neurogenic thoracic outlet syndrome, and idiopathic brachial plexopathy (also known as neuralgic amyotrophy or Parsonage-Turner syndrome)⁷.

Magnetic resonance imaging (MRI) for the brachial plexus provides a non-radiative and noninvasive method for assessing the preganglionic and post-ganglionic lesions. Past researches have showed that for the evaluation of BPI, MRI provides more information than electromyography, ultrasound, or intraoperative somatosensory-evoked potentials.^{8,9} With a higher signal-to-noise ratios and spatial resolution than low magnetic field MRI systems, 3-Tesla (T) MRI systems offer better 2- and 3-dimensional picture quality for brachial plexus assessment, especially for postganglionic lesions.^{6,10}

Numerous researches have been done to study the utility of MRI in the diagnosis of BPI without making comparisons to gold-standard diagnostic techniques like surgery.^{11,12} Other researches have compared the findings from MRI scans with those from surgeries, but the majority of these used low-magnetic-field MRI equipment.¹³⁻¹⁵

A more recent imaging method called magnetic resonance neurography (MRN) makes it possible to see the peripheral nerves more clearly⁽¹⁶⁾. When compared to traditional MRI methods, MRN offers faster imaging with great resolution, allowing users to see the compact fascicular arrangement of nerves and identify various extra- and intraneural lesions. It is increasingly utilized to evaluate lesions affecting spinal nerve roots, plexus, and peripheral nerves^(17,18).

The aim of the present study was to assess the role of 3T Magnetic Resonance Imaging in evaluation of brachial plexus. The imaging findings of both traumatic and nontraumatic brachial plexopathies were evaluated and were correlated with NCV/ EMG tests and histopathological examination wherever applicable.

MATERIALS AND METHODS

The Descriptive, cross-sectional study was conducted at Dr. D. Y. Patil Medical College and Hospital and Research Centre, Pimpri, Pune. Institutional Ethical Committee (IEC) clearance was obtained before the start of the study.

Method of diagnosis: Sixty-eight patients suspected of brachial plexus pathologies who had undergone MRI from August 2020 to September 2022 were included in the study. Informed consent and written consent were obtained from all the parents/guardians. The imaging findings were correlated with the clinical findings, EMG/NCV studies, operative findings and histopathological examination wherever applicable for confirmation of the diagnosis.

MRI TECHNIQUE:

All the brachial plexus scans were performed on Siemens Magnetom Vida Magnetic Resonance Imaging (3 Tesla) with patient in supine head first position using cervical and body coils. The patient position was secured and made comfortable to prevent movement artefacts. Following sequences were

performed for brachial plexus evaluation. Contrast study with multiplanar T1FS sequences was obtained wherever indicated.

Table 1: 3T MRN protocol for evaluation of brachial plexus

Sequence	FOV	Section thickness	TR/TE ((ms)	Matrix
Coronal T2 STIR	280	3	5700/35	210x368
3D Coronal T2 STIR SPACE	350	1	3000/249	269x448
Sagittal T2 STIR	240	3.5	6180/35	15x320
Axial T1 without fat suppression	360	2	5.5/2.46	173x384
Axial STIR	350	3	4400/78	176x384
T2 sagittal	250	3	5080/108	314x448
Axial thin T2W TSE	350	3	4400/78	176x384
Axial DWI	360	1.5	24800/60	132x200

Imaging analysis

- A) The brachial plexus was evaluated level wise from roots, trunks, divisions, cords and terminal branches, using the following criterions-
- Preganglionic injury, in the form of avulsion and/or pseudomeningocele
 - Postganglionic injury in the form of thickening, nerve disruption with or without neuroma formation.
 - Presence of mass or fibrosis, with their imaging characteristics.
- B) Level wise analysis of disc compression, their types and location.
- C) Muscles involvement with imaging features.
- D) Spinal cord involvement.

Statistical analysis

The data was collected and compiled in an excel tracker. Standard statistical tests were applied to analyze the data. It was analyzed using IBM SPSS version 16 and Microsoft word and Microsoft excel were used to express graphs and tables. Data was expressed in frequency and percentages. The imaging findings were correlated with the clinical findings, EMG/NCV studies, operative findings and histopathological examination wherever applicable for confirmation of the diagnosis.

RESULTS

In our study of 68 patients, the most common age group found was 20-40(55.9%), followed by age more than 40(36.8%) and the least common group was age less than 20(7.3). In the 68 patients, majority were male patients (73.5%), while females were 26.5%. The most common complaint was found to be restriction of movements (66%), followed by history of trauma (50%), pain in upper limb (23%) and then weakness or loss of sensation in the upper limb (8.8%). Other lesser common presentations were neck swelling (7.3%) winging of scapula (4.4%), and thinning of deltoid (1.4%). Brachial plexus was found to be abnormal on MRI in 40 patients (58.8%). In these 40 patients, unilateral involvement was noted in 36 patients (90%) and bilateral involvement was found in 4 patients (10%).

Traumatic brachial plexopathies

In our study, root trauma comprised of pre-ganglionic (4.4%), post-ganglionic injury (11.7%) and pre plus post ganglionic injury (11.7%). Preganglionic injuries were characterized by root avulsions (23.5%) and pseudomeningocele formation (13.2%) [Fig 1 (A-D)]. Among nerve root avulsions, most

were noted at C6 root (81%), followed by C7 (62%), C5 (43.8%), C8 (50%) and lastly by T1 root (25%). Pseudomeningoceles most commonly involved C6 (55.6%) and C7 (55.6%), followed by T1 (44.4%), C5 (33.3%) and C8 (33.3%) (Table 2).

Post ganglionic injuries were characterized by nerve edema (31%), nerve disruption without neuroma formation (8.8%) and with neuroma formation (1.5%) [Fig 2 (A-C)]. Nerve edema was most frequently involved C6 (81%), C7 (66.7%), C8 (61.9%), followed by C5 (52.4%) and T1(33.3%). Nerve disruption without neuroma was seen at C6(100%) and T1(100%) roots, followed by C5(50%) and C7(50%), with least commonly at C8(16.7%). Neuroma formation was noted only in 1 case, involving C6, C7 and C8 levels (Table 3).

Furthermore, traumatic pathologies were seen at the level of trunks (25%), divisions (19.1%), cords (22%) and terminal branches (23%) (Chart 1). Commonest imaging findings were high signal intensity and thickening, seen in 38% cases involving the trunks, 31% involving the divisions, 32% involving the cords and 27.9% involving the terminal branches. Discontinuity without neuroma was noted only at the trunks level, seen in 11.8% cases. Discontinuity with neuroma formation was noted in 5.9% cases at trunk level, 1.5% cases at division and cord level each. The most common abnormality in BPI, was post ganglionic injury (26.9%), followed by mixed pre- and post-ganglionic injury (23.1%) with neuroma formation seen in 11.5% patients (Chart 2). Other findings included post traumatic pseudoaneurysm, isolated trunk injuries and post traumatic fibrosis.

Table 2: Features of Preganglionic injuries

	C5 root		C6 root		C7 root		C8 root		T1 root		Total
	n	%	n	%	n	%	n	%	n	%	
Avulsion (n=16)	7	43.8	13	81.3	10	62.5	8	50.0	4	25.0	16
Pseudomeningocele (n=9)	3	33.3	4	55.6	4	55.6	3	33.3	4	44.4	9

Table 3: Features of Post-ganglionic injuries

	C5		C6		C7		C8		T1		Total
	n	%	n	%	n	%	n	%	n	%	
Nerve oedema	11	52.4	17	81.0	14	66.7	13	61.9	7	33.3	21
Nerve disruption (without neuroma)	3	50.0	6	100.0	3	50.0	1	16.7	6	100.0	6
Neuroma formation	-	-	1	100.0	1	100.0	1	100.0			1

Chart 1: Level wise distribution of MRI findings in brachial plexus abnormalities (excluding roots)

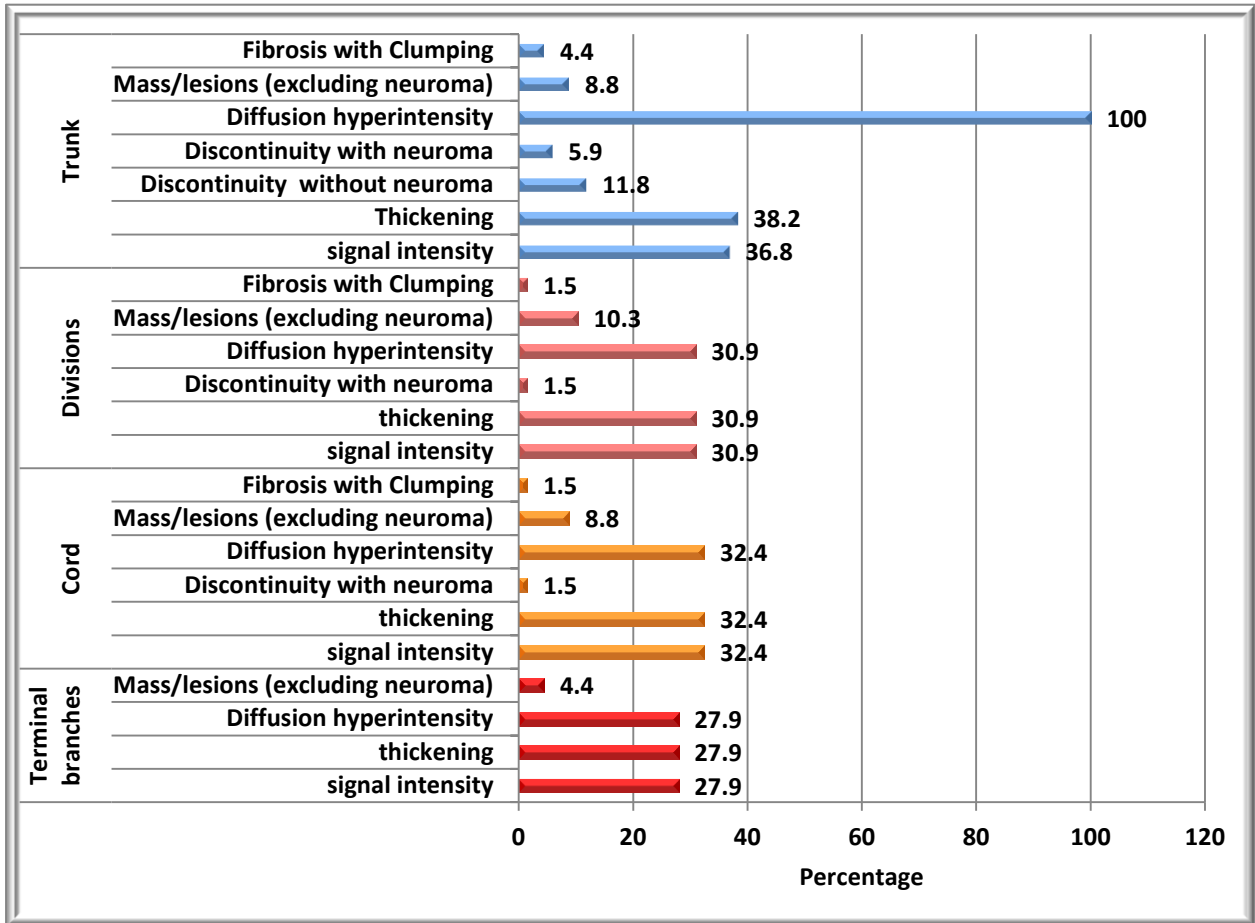
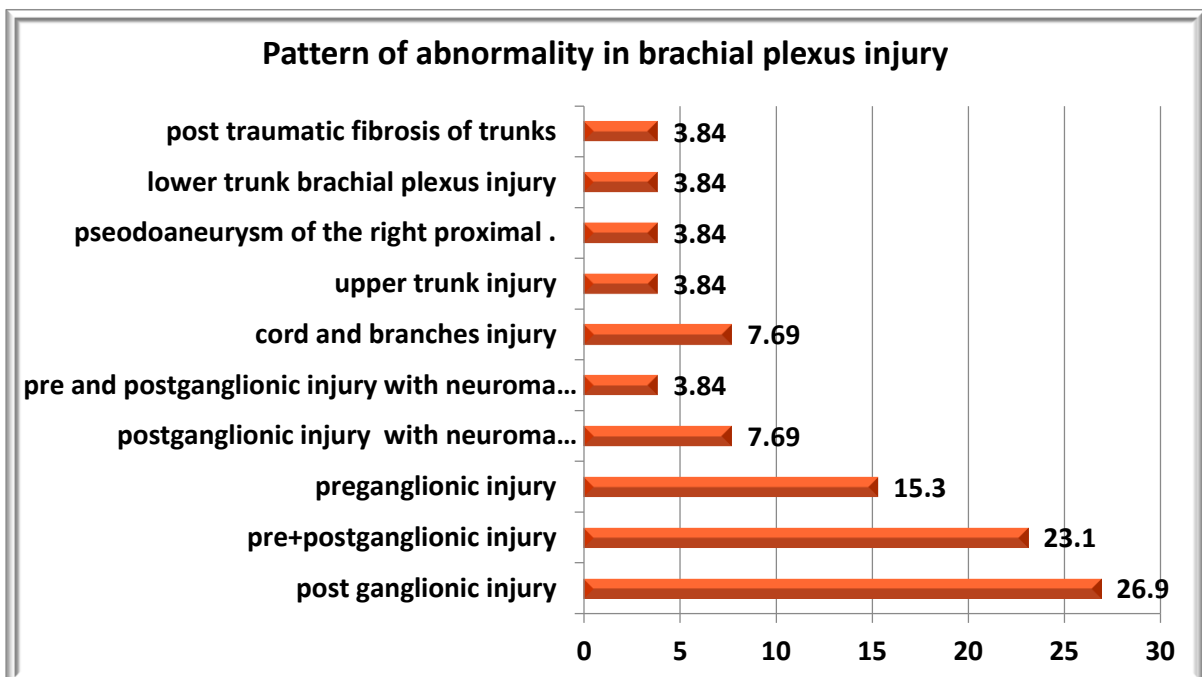


Chart 2: Pattern of abnormalities in patients with brachial plexus injury



Non traumatic brachial plexopathies

Among non-traumatic brachial plexopathies, we studied disc compression, parsonage turner syndrome, brachial plexus masses and radiation fibrosis.

Disc compression was seen in 33.8% cases among which, majority were diffuse disc bulges (82%) and remaining were protrusions (30%) (Table 4). Most commonly involved levels were C4-C5, followed by C5-C6 and C6-7 level. Among protrusion, paracentral protrusion was most commonly seen [Fig 3 (A-B)]. Out of the 23 cases of disc compression, 9-disc herniation (39.1%) correlated with the patients' symptoms while 14 cases (60.9%) did not. This finding was statistically significant with p value of <0.001.

Parsonage turner syndrome [Fig 4 (A-B)] was seen in 9 cases (13.2%), with 100% involvement of supraspinatus and infraspinatus muscles, followed by deltoid (44.4%), teres minor (44.4%) and subscapularis (44.4%) (Table 5).

Brachial plexus masses were seen in 7 cases, among which 5 were peripheral nerve sheath tumors i.e., schwannomas (42.8%) [Fig 5 (A-D)], neurofibromatosis (28.5%) [Fig 6 (A-C)] and 2 were metastatic infiltration from other primary tumors (28.5%) [Fig 7 (A-C)].

Fibrosis with clumping was seen in three cases (4.4%), involving root level in 2.9% cases, trunk level in 4.4% and divisions and cord level in 1.5% cases each, with aetiology being post traumatic, post operative and post radiation fibrosis.

Table 4: Features of disc compression

Type of herniation	Number (n=68)	Percentage	Disc involved		
			C4-C5	C5-C6	C6-C7
Diffuse bulge	19	27.9	16 (84.20)	16 (84.20)	9 (47.4)
Protrusion	7	10.3	7 (100.0)	7 (100.0)	2 (28.6)
Distribution of disc herniation (n=23)					
Diffuse bulge	19	82(19/23)	16(69.56)	16(69.56)	9(39.13)
Central Protrusion	3	13 (3/23)	3 (13.0)	3(13.0)	1 (4.34)
Paracentral Protrusion	5	21.73 (5/23)	5 (21.73)	5 (21.73)	2 (8.69)
Foraminal Protrusion	4	17.39(4/23)	4 (17.39)	4 (17.39)	1 (4.34)

Table 5: Muscle involvement in Parsonage Turner Syndrome (n=9).

Parsonage turner	Oedema		Atrophy with fatty infiltration		Oedema + Atrophy	
	n	%	n	%	n	%
Supraspinatus	8	88.9	3	33.3	1	11.1
Infraspinatus	8	88.9	3	33.3	1	11.1
Deltoid	4	44.4	1	11.1	0	0.0
Teres minor	4	44.4	3	33.3	0	0.0
Subscapularis	4	44.4	3	33.3	0	0.0

MRI correlation with NCV/EMG studies (Table 6)

Out of 68 patients, NCV/EMG studies were available in 48 patients. MRI was able to pick up 36 out of 38 abnormal NCV cases with a sensitivity of 94.7%. In one case of parsonage turner syndrome,

MRI was found abnormal, however NCV was normal. Two cases with positive NVC, had normal MRI findings. Nine cases had both normal NCV and MRI findings giving a specificity of 90%.

Table 6: Correlation between NCV/EMG (wherever applicable) and MRI findings

MRI	NCV		Total
	Abnormal	Normal	
Abnormal	36	1	37
Normal	2	9	11
Total	38	10	48

DISCUSSION

Our study predominantly consisted of male patients constituting 73.5%, while females were 26.5%. According to Midha et al³, the prevalence of traumatic brachial plexopathy is higher among men because they participate in more sporting events and motorcycle rides. In our study of 68 patients, the most common complaint was found to be restriction of movements (66%). Thirty four out of our 68 patients came with history of trauma, majority of which were caused by road traffic accidents and falls. This was in concordance with study conducted by Vinoth T et al¹⁹ in which 53% of their cases presented with brachial plexopathy following trauma. It was followed by upper limb pain (23%) and radiculopathy (8.8%). Five cases (7.3%) presented with neck swellings, which were diagnosed as peripheral nerve sheath tumours or metastases. Out of the 68 patients, brachial plexus was found to be abnormal on MRI in 40 patients (58.8%). In these 40 patients, unilateral involvement was noted in 36 patients (90%) and bilateral involvement was found in 4 patients (10%). In their study, Mauricio Castillo et al²⁰ noted that not every patient referred for brachial plexus injuries had abnormal findings; in fact, roughly 40% of patients had normal results as well.

Traumatic Brachial plexus injuries

In our study, root trauma comprised of pre-ganglionic (4.4%), post-ganglionic injury (11.7%) and pre plus post ganglionic injury (11.7%). Preganglionic injuries were characterized by root avulsions (23.5%) and pseudomeningocele formation (13.2%). Among nerve root avulsions, most were noted at C6 root (81%), followed by C7 (62%), C8 (50%), C5 (43.8%), and lastly by T1 root (25%). Pseudomeningoceles most commonly involved C6 (55.6%) and C7 (55.6%), followed by T1 (44.4%), C5 (33.3%) and C8 (33.3%). This was slightly different from the findings in study by Wade et al who observed that root avulsions and pseudomeningoceles were mostly seen at the C7 and C8 roots, with detection rates of 60% and 40%, respectively.⁴ Based on their 57% detection rate, Hung et al²¹ in a study of 60 patients with suspected brachial plexus injuries determined that pseudomeningocele and root avulsion more frequently occurred at the C7 (30%) and C8 (29.5%) roots with C6 (14.5%) nerve root being less commonly involved. High rates of root avulsions at C7 and C8 are likely caused by the lack of ligaments supporting these roots in the spinal foramina²². In our study, C7 and C8 nerve roots avulsion was also seen in more than 50% of traumatic nerve root avulsions; however, C6 was the most common nerve root involved.

We characterized the post ganglionic injuries by nerve edema or thickened nerves (31%), nerve disruption without neuroma formation (8.8%) and with neuroma formation (1.5%). Nerve edema was most frequently involved C6 (81%), C7 (66.7%), C8 (61.9%), followed by C5 (52.4%) and T1 (33.3%) nerve roots. Nerve disruption without neuroma was seen at C6 (100%) and T1(100%) roots, followed by C5(50%) and C7(50%), with least commonly at C8(16.7%). Neuroma formation was noted only in 1 case, involving C6, C7 and C8 levels. Nerve stem thickness²¹ and hyperintensity are the most frequent MRI characteristics in post-ganglionic injuries of the brachial plexus, according to researchers. Zhang L. et al²³ studied 28 patients with BPIs, found that in post ganglionic injuries, nerve thickening with hyperintense signal due to rising water content in tissues under edema and

inflammation was observed in 47.0% of cases, and total nerve rupture (34.7%) was observed in 34.7% of cases. Also, 7.1% of patients with late-stage brachial plexus injuries accompanied by local nerve bleeding and fibrosis developed post-traumatic fibrosis in their study. Zhang et al²³ also reported pseudo-neuromas forming due to contracture of the damaged nerve fibers, muscle atrophy, hyperintense signal, and structural disruption and soft tissue edoema around an injured neuron. Muscle atrophy, brought on by nerve damage, could set in over time. Commonest imaging findings in our study were high signal intensity and thickening, seen in 38% cases involving the trunks, 31% involving the divisions, 32% involving the cords and 27.9% involving the terminal branches. Discontinuity without neuroma was noted only at the trunks level, seen in 11.8% cases. Discontinuity with neuroma formation was noted in 5.9% cases at trunk level, 1.5% cases at division and cord level each. One case with one year old history of trauma, showed clumping in the region of the trunks of brachial plexus, which was given a diagnosis of post traumatic fibrosis.

Disc compression of brachial plexus nerve roots

Out of the 68 patients, 17 patients had isolated had disc compression (25%), 20 patients (29.4) had pathologies excluding disc compression and 6 patients (8.8%) had both disc compression and other pathologies. Among the disc compression, majority were diffuse disc bulges (82%) and remaining were protrusions (30%). This was in concordance with the study conducted by Siddharth MC et al²⁴, who studied disc compression in 70 patients and found that diffuse disc bulges were seen in 54% cases, central disc extrusion was seen in 4.2% and paracentral disc extrusion was seen in 9.7% cases.

The disc bulges were most commonly noted at C4-C5 (69.5%) and C5-C6 (69.5%) levels, followed by C6-7 level (39.1%). Among the disc protrusions, most common was paracentral protrusion, noted in 5 cases (21.7%), predominantly seen at C4-C5 (21.7%), C5-C6 (21.7%) and C6-7 level (8.6%), followed by 4 cases of foraminal protrusions (17.3%), seen at C4-C5 (17.3%) and C5-C6 (17.3%) levels, followed by C6-7 level (4.3%) and 3 cases of central protrusion (13%) at C4-C5 (13%) and C5-C6 (13%) levels, followed by C6-7 level (4.3%).

Siddharth MC et al.²⁴ also observed that disc bulges were most common at the C5-C6 level, followed by the C6-C7 level (72%), the C4-C5 level (60%), the C3-C4 level (38%), the C2-C3 level (22%), and the C7-T1 level (13%). Paracentral disc extrusion was seen most frequently at the C5-C6 level (12%), then at the C6-C7 level (12%), then at the C4-C5 level (12%), and finally at the C3 level (3%) in their study. Also, the most common level for central disc extrusion was C5-C6, followed by C6-C7 (4%), and C4-C5 (2%).

It was found by Crock HR et al.²⁵ that the most disc protrusion were seen at C6-C7 and C5-C6 (90%) levels, with very few at C4-C5 (7%), C3-C4 (3%), and C7-T1 (1%) levels.

Parsonage turner syndrome

In the 9 cases of Parsonage turner syndrome, we found that the commonest muscles involved were supraspinatus (100%), and infraspinatus (100%), followed by deltoid (44.4%), teres minor (44.4%) and subscapularis (44.4%). Recent studies²⁶ show that the suprascapular nerve, branch of the brachial plexus's superior trunk, is the most common site for anomalies on EMG in Parsonage-Turner syndrome. This is consistent with our findings, which revealed that the supraspinatus and infraspinatus muscles, both innervated by the suprascapular nerve, were the most commonly involved. Scalf et al²⁷ also studied of 26 patients diagnosed with Parsonage turner syndrome and found that the supraspinatus and infraspinatus muscles were most commonly involved. Out of the 9 cases of parsonage, 3 (33%) were found to have bilateral involvement, which was similar with the previous researches^{28,29,30}, which revealed that 10%-30% of people with brachial plexus neuritis also experienced bilateral involvement.

The signal intensity of muscles can be normal on MRI during the acute phase of denervation. The first detectable change in denervated muscles is diffuse increased T2-weighted signal (due to edoema), which may occur in the absence of a change in T1-weighted signal^{31,32,33}. T2-weighted signal

abnormalities persist in the subacute and chronic phases of denervation, and muscular atrophy may develop³¹. Muscle atrophies are characterized by decreased muscular mass and fatty infiltration attributing to increased intramuscular, linear, T1-weighted signal³⁴. In our study, both supraspinatus and infraspinatus muscles showed denervation edema (88.9%), atrophy with fatty replacement (33.3%) and atrophy with edema (11.1%). Other shoulder muscle groups, such as the latissimus dorsi and rhomboid, may also exhibit abnormal MRI signal changes²⁷. Some of the cases with denervation edoema in our study involved the teres minor muscle (4%) and the subscapularis muscle (4%).

We also studied the pattern of muscle involved in all brachial plexopathies, and found that the most common finding was denervation edema (23.5%), followed by muscle atrophy with fatty infiltration (20.6%) and lastly by muscle atrophy with edema (4.4%). Among the 30 cases with muscle involvement, 20 were seen in patients with history of trauma, 9 in patients diagnoses as Parsonage turner syndrome and 1 in the case of post radiation fibrosis.

Brachial plexus masses

Benign nerve sheath tumors, such as schwannomas, neurofibromas, and their malignant forms, are the most prevalent primary tumors of the brachial plexus. In our study, 7 cases had brachial plexus masses among which 5 were peripheral nerve sheath tumors i.e. schwannomas (42.8%), neurofibromatosis (28.5%) and 2 had metastatic infiltration from other primary tumors (28.5%). Schwannomas were seen as well defined, ovoid, enhancing, encapsulated lesion in continuity with the nerves. Neurofibromatosis was seen as multiple lobulated well-defined intensely enhancing extra dural lesions along the nerves. All the three schwannomas were noted involving the trunks, divisions and cords(supraclavicular), with two of them involving the terminal branches (infraclavicular) also. Neurofibromatosis was noted involving bilateral pan brachial plexus in one case and isolated terminal branches in other. This was in concordance with previous studies. Desai KI et al³⁵ reported that supraclavicular tumours involving the roots and trunks occurred in 61.7% cases, whereas infraclavicular tumours involving the cords and branches occurred in 38.2 cases. According to Go MH³⁶, 15 tumours (68.18%) were supraclavicular, while 3 tumours (13.64%) were infraclavicular and the remaining 4 tumours (18.18%) were both supraclavicular and infraclavicular. According to X. Jia et al,³⁷ trunks are the most commonly involved part in primary brachial plexus tumours.

Metastatic infiltration of the brachial plexus is most frequently seen in patients with breast or lung carcinoma. Breast carcinoma metastases, the most common primary, typically travel to the plexus through the lymphatic system. Some cases of brachial plexopathy have been linked to metastasis from melanoma and gastrointestinal or genitourinary carcinomas that have spread to nearby lymph nodes, soft tissue, or bone^{38,39,40}. Primary in one our case was squamous cell carcinoma of buccal mucosa and other was unknown primary. Metastases was found to involve roots, divisions and cords in one case and just cords in another case.

Brachial plexus fibrosis

Radiation plexopathy, which affects the infraclavicular plexus, can develop anywhere from a few months to 20 years after the start of therapy (incidence: 5%–10%)⁴¹. These pathologies are common in the C-5C-8 levels but uncommon in T1 vertebrae.⁴² According to Bilbey et al,⁴³ T2-weighted images of delayed radiation injury or fibrosis typically show iso or hypointense lesion in comparison to muscle. However, Wouter et al⁴⁴ pointed out that T2WI exhibited mild to moderate hyperintensity in the brachial plexus edoema and diffuse infiltration by fibrosis.

In our study, fibrosis with clumping was seen in three cases (4.4%), involving root level in 2.9% cases, trunk level in 4.4% and divisions and cord level in 1.5% cases each. One female patient had history of radiotherapy for breast carcinoma, she presented 1 year later to our department with upper limb radiculopathy, and demonstrated thickened and clumped nerve roots, trunks, divisions and cords. Another patient underwent cervical rib excision and presented 1 year later with upper limb pain, was found to have thickened and clumped nerve roots and trunks, which was given a diagnosis of post

operative fibrosis. Also, patients with late-stage brachial plexus injuries accompanied by local nerve bleeding and fibrosis can develop post-traumatic fibrosis²³. One case in our study, with one year old history of trauma, showed clumping in the region of the trunks of brachial plexus, which was given a diagnosis of post traumatic fibrosis.

NCV and MRI correlation

In our study, NCV/EMG studies were available in 48 patients. We found that MRI was able to pick up 36 out of 38 abnormal NCV cases with a sensitivity of 94.7%. In one case of parsonage turner syndrome, MRI was found abnormal, however NCV was normal. Two cases with positive NVC, had normal MRI findings. Nine cases had both normal NCV and MRI findings giving a specificity of 90%. This was in line with research by Mabrouk et al,⁴⁵ who discovered that there was good agreement between NCV/EMG studies and MRN, and that the latter's sensitivity and specificity were 94.44% and 100%, respectively, when it came to comparing its findings to those of clinical exams and electrophysiological studies. Similar results were found when comparing electrodiagnostic tests with MRN by Fisher et al,⁴⁶ who found that in 31 of 47 cases (66.0%), the ED tests coincided with the MRN results. Du et al⁴⁷ discovered that when MRN was compared with EMG/NCS, MRN provided the same data in 29 patients (32%), extra info in 41 (45%), less info in 15 (17%), and a different diagnosis in 6 (7%).

CONCLUSION

In conclusion, 3T MRI is the highly accurate, reliable and preferred method for brachial plexus pathology evaluation. MR neurography study with quick image acquisition and high resolution make it possible to find both extra-neural and intraneural pathologies of the brachial plexus. MR imaging is crucial in evaluating traumatic brachial plexopathy and plays an important role in localizing and differentiating between preganglionic and postganglionic injury. It also helps to further characterize the injury by demonstrating neural stretching, rupture, or nerve avulsion with or without neuroma formation which helps the clinician in treatment planning. MRI is important in evaluation of non-traumatic brachial plexopathies caused by disc compression, neurogenic tumors, Parsonage Turner Syndrome, extrinsic compression or infiltration by localised pathologies like neoplasia/metastases and fibrosis. MRI also has good correlation with electrodiagnostic tests and offers high sensitivity and specificity for diagnosis of brachial plexopathies. Brachial plexus pathology may be better evaluated and localised with the help of MRN when electrodiagnostic tests are negative or inconclusive, as opposed to only relying on the clinical exam alone.

Figures:

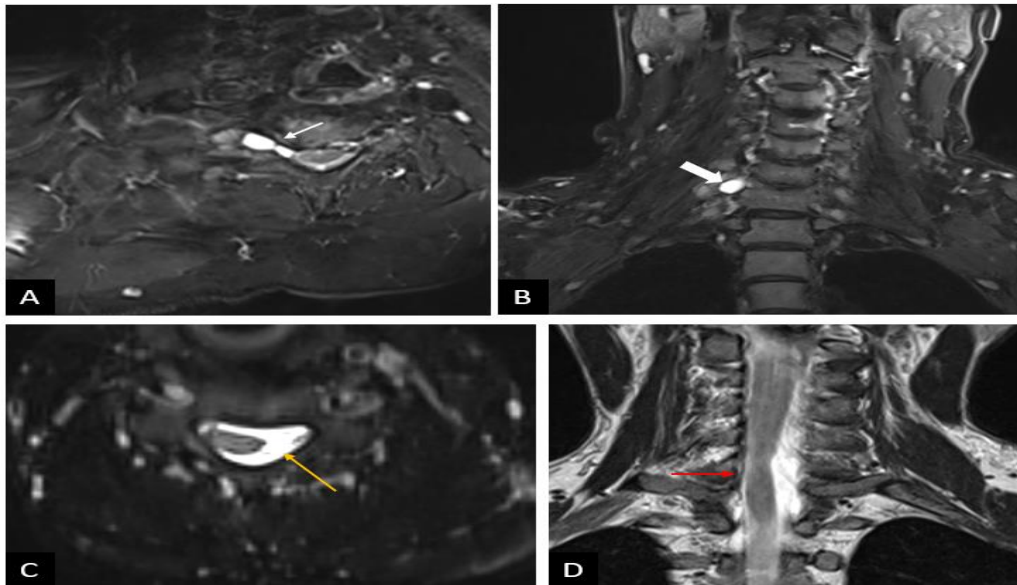


Fig 1 (A-D): Preganglionic brachial plexus injury with pseudomeningocele in a 52-year-old male patient with history of road traffic accident. T2 STIR axial (A) and coronal (B) MR images reveal C7 nerve root avulsion on the left side (Thin white arrow) with CSF intensity outpouching of the C7 nerve sheath through the neural foramen compatible with a pseudomeningocele (Thick white arrow). T2 space axial (C) and T2 coronal (D) MR images of another patient show a pseudomeningocele with the detached nerve root within it. (D) Contralateral deviation of the spinal cord (red arrow) is also seen in the same patient which is an indirect sign of preganglionic injury.

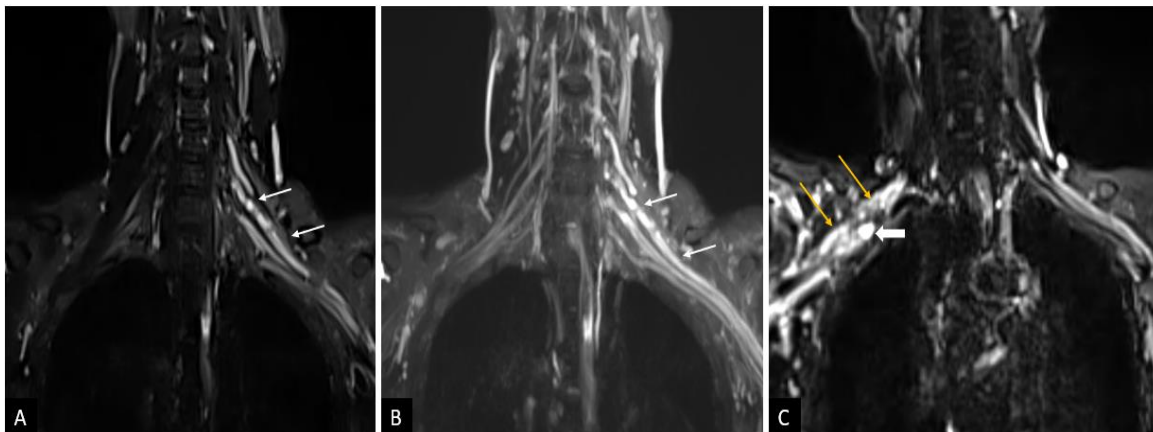


Fig 2 (A-C): Post ganglionic brachial plexus injuries in 32-year-old male patient with history of road traffic accident (A, B). T2 SPACE STIR coronal (A) and MIP (B) MR images show diffuse thickening with increased hyperintensities in the post-ganglionic part of C5 to C8 nerve roots, trunks, divisions and visualized cords of these roots on the left side (thin white arrows). T2 SPACE STIR coronal MR image (C) of another patient with history of road traffic accident shows bulky trunks, divisions and cords of the right brachial plexus with edema (thin orange arrows) and focal discontinuity just after scalene triangle resulting in neuroma (Thick white arrow)– representing post ganglionic injury with neuroma formation.

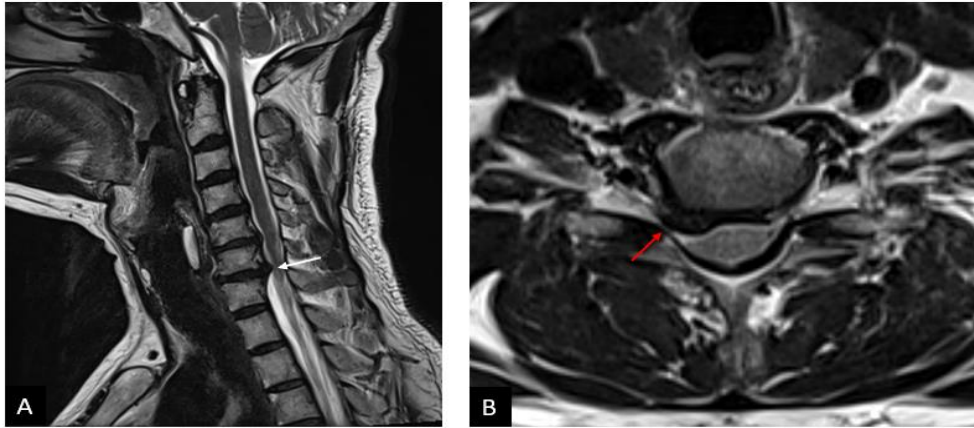


Fig 3 (A-B): Disc protrusion causing root compression in 52-year-old female patient with complaints of right upper limb radiculopathy. T2 sagittal (A) and axial (B) MR images show right paracentral- right foraminal protrusions of C6-7 disc is seen indenting the anterior cord surface (white arrow) and compressing the right exiting C7 nerve root (red arrow).

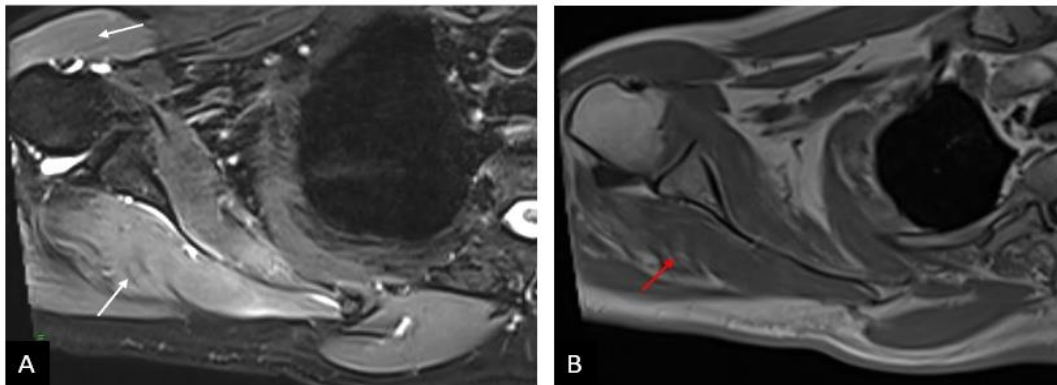


Fig 4 (A-B): Parsonage Turner Syndrome in male patient with right upper limb radiculopathy. T2 STIR axial MR image (A) show hyperintense signal in the supraspinatus, infraspinatus and deltoid likely suggestive of muscle edema. T1W axial MR image (B) show mild atrophy with fatty infiltration (red arrow) of supraspinatus and infraspinatus muscle.

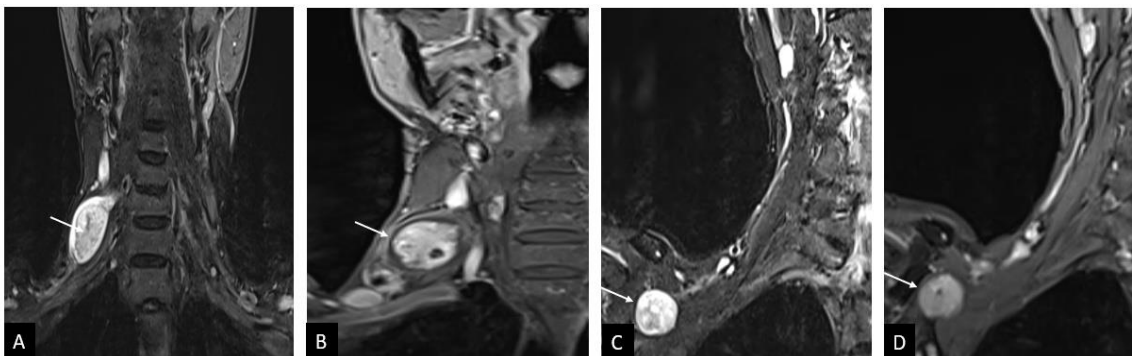


Fig 5 (A-D): Schwannoma in 70-year-old male patient with painful neck swelling. T2 STIR coronal(A), T1 post contrast coronal(B) MR images reveal a well defined, ovoid, enhancing, encapsulated lesion (white arrows) in the right side of neck in supraclavicular region at C6-C7 vertebral levels in continuity with the right C6 exiting nerve root. Similar lesion is seen along the right brachial plexus in right infraclavicular region in T2 STIR coronal(C), T1 post contrast coronal(D) MR images.

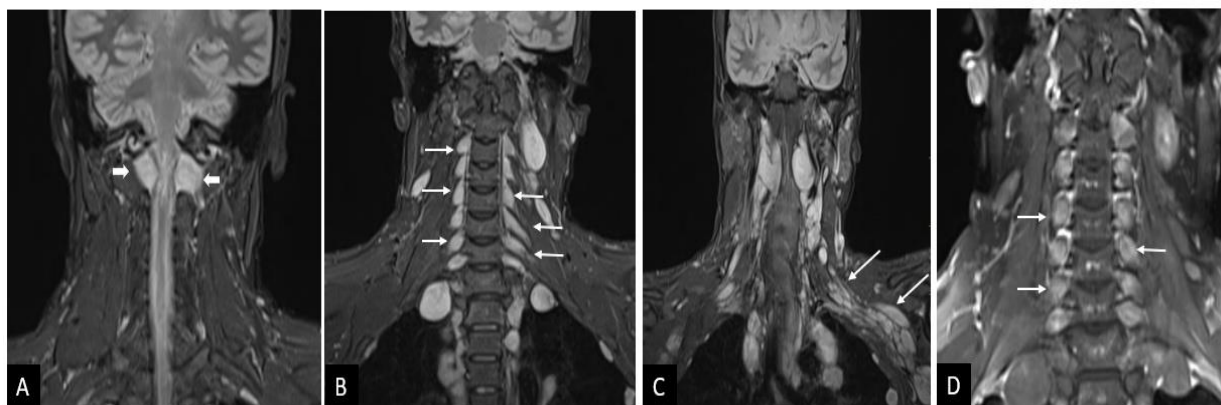


Fig 6 (A-C): Plexiform neurofibromatosis in 30-year-old male with pain and radiculopathy of the left lower limb. T2 STIR coronal MR image (A) shows two well-defined extra dural lesions (thick white arrows) are seen along the exiting nerve roots at C1-2 level causing widening of bilateral neural foramina and significant compression of the cervical cord just distal to cervicomedullary junction resulting in marked myelomalacia. T2 STIR coronal (B, C) and T1 post contrast coronal (D) MR images show multiple lobulated lesions (thin white arrows) of similar signal intensity and of variable sizes along the extra foraminal exiting nerve roots and their branches at all cervical levels and visualized upper thoracic spine, involving the brachial plexus and intercostal nerves bilaterally.

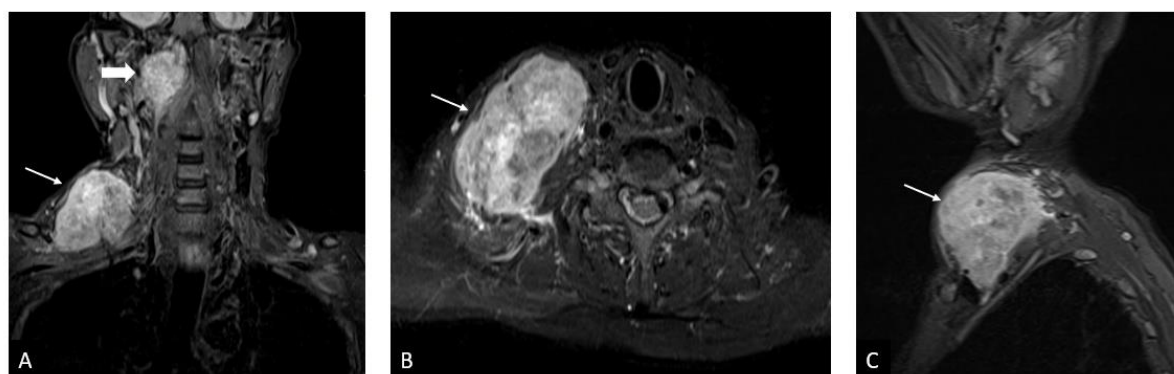


Fig 7 (A-C): Metastases involving right brachial plexus in a 66-year-old male with neck swelling with an unknown primary. T2 STIR coronal (A), axial (B) and sagittal (C) MR images show a lesion (white arrows) in right supraclavicular region involving the trunks, divisions, cords and proximal part of terminal branches of the right brachial plexus. Another lesion (Thick white arrow) can be seen as a lobulated lesion involving right craniovertebral junction, right transverse process and anterior arch of C1 vertebra (A).

REFERENCES

1. Gerevini S, Mandelli C, Cadioli M, Scotti G. Diagnostic value and surgical implications of the magnetic resonance imaging in the management of adult patients with brachial plexus pathologies. *Surgical and Radiologic Anatomy*. 2008 Mar;30(2):91-101.
2. Bowen BC, Pattany PM, Saraf-Lavi E, Maravilla KR. The brachial plexus: normal anatomy, pathology, and MR imaging. *Neuroimaging Clinics*. 2004 Feb 1;14(1):59-85.
3. Midha R. Epidemiology of brachial plexus injuries in a multitrauma population. *Neurosurgery* 1997; 40(6): 1182–1189.
4. Wade RG, Itte V, Rankine JJ, et al. The diagnostic accuracy of 1.5T magnetic resonance imaging for detecting root avulsions in traumatic adult brachial plexus injuries. *J Hand Surg Eur* 2018; 43(3): 250–258.

5. Yang J, Qin B, Fu G, et al. Modified pathological classification of brachial plexus root injury and its MR imaging characteristics. *J Reconstr Microsurg* 2013; 30(3): 171–178.
6. Qin BG, Yang JT, Yang Y, et al. Diagnostic value and surgical implications of the 3D DW-SSFP MRI on the management of patients with brachial plexus injuries. *Sci Rep* 2016; 6(1):35999.
7. Nwawka OK. Ultrasound imaging of the brachial plexus and nerves about the neck. *Ultrasound Quarterly*. 2019 Jun 1;35(2):110-9.
8. Lapegue F, Faruch-Bilfeld M, Demondion X, et al. Ultrasonography of the brachial plexus, normal appearance and practical applications. *Diagn Interv Imaging* 2014; 95(3):259–275.
9. O’Shea K, Feinberg JH, and Wolfe SW. Imaging and electrodiagnostic work-up of acute adult brachial plexus injuries. *J Hand Surg Eur* 2011; 36(9): 747–759.
10. Chhabra A, Thawait GK, Soldatos T, et al. High-resolution 3T MR neurography of the brachial plexus and its branches, with emphasis on 3D imaging. *AJNR Am J Neuroradiol* 2013;34(3): 486–497.
11. Takahara T, Hendrikse J, Yamashita T, et al. Diffusion-weighted MR neurography of the brachial plexus: Feasibility study. *Radiology* 2008; 249(2): 653–660.
12. Qiu TM, Chen L, Mao Y, et al. Sensorimotor cortical changes assessed with resting-state fMRI following total brachial plexus root avulsion. *J Neurol Neurosurg Psychiatry* 2014; 85(1): 99–105.
13. Carvalho GA, Nikkiah G, and Samii M. Diagnosis and surgical indications of traumatic brachial plexus lesions from the neurosurgery viewpoint. *Orthopade* 1997; 26(7):599–605.
14. Hems TEJ, Birch R, and Carlstedt T. The role of magnetic resonance imaging in the management of traction injuries to the adult brachial plexus. *J Hand Surg* 1999; 24(5):550–555.
15. Chanlalit C, Vipulakorn K, Jiruttanapochai K, et al. Value of clinical findings, electrodiagnosis and magnetic resonance imaging in the diagnosis of root lesions in traumatic brachial plexus injuries. *J Med Assoc Thai* 2005; 88(1): 66–70.
16. Truong MT, Nadgir RN, Hirsch AE, Subramaniam RM, Wang JW, Wu R, Khandekar M, Nawaz AO, Sakai O. Brachial plexus contouring with CT and MR imaging in radiation therapy planning for head and neck cancer. *Radiographics*. 2010 Jul;30(4):1095-103.
17. Hassan HG, Bassiouny RH, Mohammad SA. Quantitative MR neurography of brachial plexus lesions based on diffusivity measurements. *The Egyptian Journal of Radiology and Nuclear Medicine*. 2018 Dec 1;49(4):1093-102.
18. Aagaard BD, Maravilla KR, Kliot M. Magnetic resonance neurography: magnetic resonance imaging of peripheral nerves. *Neuroimaging clinics of North America*. 2001 Feb 1;11(1):viii-131.
19. T DV. Role of MRI in Correlation with NCS in Brachial Plexopathies. *Journal of Medical Science And clinical Research*. 2016 Nov 29;04(11):14277–80.
20. Castillo M. Imaging the anatomy of the brachial plexus: review and self-assessment module. *American Journal of Roentgenology*. 2005 Dec;185(6_supplement):S196-204.
21. Hung ND, Duc NM, Xoan NT, Doan NV, Huyen TTT, Dung LT. Diagnostic Function of 3- Tesla Magnetic Resonance Imaging for the Assessment of Brachial Plexus Injury. *Ann Neurosci*. 2020 Jul;27(3-4):124-130.
22. Acharya AM, Cherian BS, Bhat AK. Diagnostic accuracy of MRI for traumatic adult brachial plexus injury: A comparison study with surgical findings. *Journal of Orthopaedics*. 2020 Jan 1;17:53-8.
23. Zhang L, Xiao T, Yu Q, Li Y, Shen F, Li W. Clinical value and diagnostic accuracy of 3.0 T multi-parameter magnetic resonance imaging in traumatic brachial plexus injury. *Medical science monitor: international medical journal of experimental and clinical research*. 2018;24:7199.
24. Siddharth MC et al., 2018, Role of Mri in Evaluation of Non Traumatic Causes of Brachial Plexus Pathologies. *Int J Recent Sci Res*. 9(10), pp. 29233-29241.

25. Crock HV. The presidential address: ISSLS: Internal disc disruption a challenge to disc prolapse fifty years on. *Spine*. 1986 Jul 1;11(6):650-3.
26. Beghi E, Kurland LT, Mulder DW, Nicolosi A. Brachial plexus neuropathy in the population of Rochester, Minnesota, 1970–1981. *Annals of Neurology: Official Journal of the American Neurological Association and the Child Neurology Society*. 1985 Sep;18(3):320-3.
27. Scalf RE, Wenger DE, Frick MA, Mandrekar JN, Adkins MC. MRI findings of 26 patients with Parsonage-Turner syndrome. *AJR Am J Roentgenol*. 2007 Jul;189(1):W39-44.
28. Parsonage MJ, Turner JA. Neuralgic amyotrophy the shoulder-girdle syndrome. *The Lancet*. 1948 Jun 26;251(6513):973-8.
29. Tsairis P, Dyck PJ, Mulder DW. Natural history of brachial plexus neuropathy: report on 99 patients. *Archives of Neurology*. 1972 Aug 1;27(2):109-17.
30. Gaskin CM, Helms CA. Parsonage-Turner syndrome: MR imaging findings and clinical information of 27 patients. *Radiology*. 2006 Aug;240(2):501-7.
31. Uetani M, Hayashi K, Matsunaga N, Imamura K, Ito N. Denervated skeletal muscle: MR imaging. Work in progress. *Radiology*. 1993 Nov;189(2):511-5.
32. Fleckenstein JL, Watumull D, Conner KE, Ezaki M, Greenlee Jr RG, Bryan WW, Chason DP, Parkey RW, Peshock RM, Purdy PD. Denervated human skeletal muscle: MR imaging evaluation. *Radiology*. 1993 Apr;187(1):213-8.
33. West GA, Haynor DR, Goodkin R, Tsuruda JS, Bronstein AD, Kraft G, Winter T, Kliot M. Magnetic resonance imaging signal changes in denervated muscles after peripheral nerve injury. *Neurosurgery*. 1994 Dec 1;35(6):1077-86.
34. Shabas D, Gerard G, Rossi D. Magnetic resonance imaging examination of denervated muscle. *Computerized radiology*. 1987 Jan 1;11(1):9-13.
35. Desai KI. Primary benign brachial plexus tumors: an experience of 115 operated cases. *Neurosurgery*. 2012 Jan 1;70(1):220-33.
36. Go MH, Kim SH, Cho KH. Brachial plexus tumors in a consecutive series of twenty one patients. *Journal of Korean Neurosurgical Society*. 2012 Aug 31;52(2):138-43.
37. Jia X, Yang J, Chen L, Yu C. Large cervicothoracic myxoinflammatory fibroblastic sarcoma with brachial plexus invasion: A case report and literature review. *Oncology Letters*. 2016 Sep 1;12(3):1717-20.
38. Kori SH, Foley KM, Posner JB. Brachial plexus lesions in patients with cancer= 100 cases. *Neurology*. 1981 Jan 1;31(1):45-.
39. de Verdier HJ, Colletti PM, Terk MR. MRI of the brachial plexus: a review of 51 cases. *Computerized medical imaging and graphics*. 1993 Jan 1;17(1):45-50.
40. Posniak HV, Olson MC, Dudiak CM, Wisniewski R, O'Malley C. MR imaging of the brachial plexus. *AJR. American journal of roentgenology*. 1993 Aug;161(2):373-9.
41. Chhabra A, Ashikyan O, Slepicka C, Dettori N, Hwang H, Callan A, Sharma RR, Xi Y. Conventional MR and diffusion-weighted imaging of musculoskeletal soft tissue malignancy: correlation with histologic grading. *European Radiology*. 2019 Aug;29(8):4485-94.
42. Cai Z, Li Y, Hu Z, Fu R, Rong X, Wu R, Cheng J, Huang X, Luo J, Tang Y. Radiation-induced brachial plexopathy in patients with nasopharyngeal carcinoma: a retrospective study. *Oncotarget*. 2016 Apr 4;7(14):18887.
43. Bilbey JH, Lamond RG, Mattrey RF. MR imaging of disorders of the brachial plexus. *Journal of Magnetic Resonance Imaging*. 1994 Jan;4(1):13-8.
44. van Es HW, Engelen AM, Witkamp TD, Ramos LM, Feldberg MA. Radiation-induced brachial plexopathy: MR imaging. *Skeletal radiology*. 1997 May;26(5):284-8.

45. Mabrouk SM, Zaytoon HA, Farid AM, Khadrah RS. Additive value of magnetic resonance neurography in diagnosis of brachial plexopathy: a cross-section descriptive study. *Egyptian Journal of Radiology and Nuclear Medicine*. 2021 Dec;52(1):1-8.
46. Fisher S, Wadhwa V, Manthuruthil C, Cheng J, Chhabra A. Clinical impact of magnetic resonance neurography in patients with brachial plexus neuropathies. *The British Journal of Radiology*. 2016 Nov;89(1067):20160503.
47. Du R, Auguste KI, Chin CT, Engstrom JW, Weinstein PR. Magnetic resonance neurography for the evaluation of peripheral nerve, brachial plexus, and nerve root disorders. *Journal of neurosurgery*. 2010 Feb 1;112(2):362-71.